DOI: https://doi.org/10.14311/TPFM.2023.021

RUNGE-KUTTA DISCONTINUOUS GALERKIN METHOD APPLIED TO SHALLOW WATER EQUATIONS

C. Poussel [1], M. Ersoy [1], F. Golay [1], Y. Mannes [1]

[1] **Université de Toulon, IMATH, EA 2137, 83957 La Garde, France**

Abstract

This work is devoted to the numerical simulation of Shallow Water Equations using Runge-Kutta Discontinuous Galerkin methods. Such methods were implemented in the framework of adaptive mesh refinement method using a block-based approach. The space and time discretization using the Runge-Kutta Discontinuous Galerkin approach is applied to nonlinear hyperbolic Shallow Water Equations. Increasing the order of approximation, spurious oscillations appear and are addressed using moment limiters. Finally, the solver is validated with a one-dimensional dam-break problem and its behavior is tested solving a two-dimensional benchmark.

Keywords: Discontinuous Galerkin method, Shallow Water Equations, Moment limiter, Non-conformal mesh.

1 Introduction

This work is developed in the framework of the interaction between the flow of water in sandy beaches and the free surface flow above the sand. Simulating the flow of groundwater has been done by Clement in 2021 [1] using the adaptive Discontinuous Galerkin method to solve Richards' equation. The present work aims at developing the hyperbolic part which will be coupled to the parabolic one.

The free surface flow over sandy beaches will be modelled using the Shallow Water Equations (SWE). They are derived by considering the depth-averaged three-dimensional incompressible Navier-Stokes Equations, assuming hydrostatic pressure distribution and neglecting vertical acceleration and viscous effects [2, 3, 4].

Spacial approximation is done using Discontinuous Galerkin (DG) methods. DG methods combine the background of Finite Element methods and Finite Volume methods, since a weak problem is solved in a Sobolev space and the solution is approximated with discontinuous polynomials. Moreover in the context of hyperbolic problems, numerical fluxes are approximated taking into account the physics of the problem. Due to the discontinuous approximation, the DG methods are well adapted to non-conformal meshing. As in Finite Volume methods, increasing the DG space approximation order introduces spurious oscillations of the numerical solutions. To counter this unwanted effect, slope limiting [5] and moment limiting [6] can be used.

DG methods were introduced in 1989 by Cockburn [5] in the scope of conservative laws and were extended to more precisely convection-dominated problems in 2001 [7]. More recently such methods were broadly used to solve SWE [8, 9, 10, 11].

The time discretization is performed using explicit Runge-Kutta (RK) method. Explicit RK method [12] is well suited for DG methods, because the order can be increased easily. The time adaptation is part of the global hp-adaptation were the time order follows the polynomial approximation [7].

The main purpose of this work is to implement a Runge-Kutta Discontinuous Galerkin (RKDG) solver using a block based adaptive mesh refinement technique (BB-AMR) [1, 13]. This paper is organized as follows. In Section 2, we recall the expression of SWE in 2D with bathymetry source term. In Section 3, we detail the space and time discretization of RKDG methods and then we add the hydrostatic reconstruction to ensure the well balanced property. Finally we introduce the moment limiter to cancel spurious oscillations. In Section 4, a one-dimensional dam-break problem is performed to validate the solver and its behavior is tested solving a two-dimensional benchmark.

2 Governing equations

Let us consider an open domain Ω, a subset of $\mathbb{R}^2$, and consider $T > 0$ be the simulation time. The gravitational acceleration is denoted by g and $z : \Omega \to \mathbb{R}$ is a smooth function representing the bathymetry. The SWE can be written as follows:

$$\begin{cases} \partial_t U + \nabla \cdot \mathbb{G}(U) = \mathbb{S}(U, z) \quad in \quad \Omega \times]0, T[, \\ \text{Initial and Boundary conditions,} \end{cases} \tag{1}$$

where $U := (\zeta, \mathbf{q}) : \Omega \times [0, T[\to \mathbb{R}^3$ are the conservatives variables, ζ is the (scalar-valued) water depth, $\mathbf{u} = (u, v)$ is the horizontal velocity and $\mathbf{q} = (q_x, q_y) = (\zeta u, \zeta v)$ is the horizontal discharge. Moreover the flux function $\mathbb{G}$ and the source trem $\mathbb{S}$ are expressed:

$$\mathbb{G}(U) := \begin{pmatrix} q_x & q_y \\ \frac{q_x^2}{\zeta} + g\frac{\zeta^2}{2} & \frac{q_x q_y}{\zeta} \\ \frac{q_x q_y}{\zeta} & \frac{q_y^2}{\zeta} + g\frac{\zeta^2}{2} \end{pmatrix}; \quad \mathbb{S}(U, z) := \begin{pmatrix} 0 \\ -g\zeta\partial_x z \\ -g\zeta\partial_y z \end{pmatrix}.$$

This problem will be solved numerically using RKDG methods.

3 Runge-Kutta Discontinuous Galerkin approach

In this section the space and time discrezation are detailed and then hydrostatic reconstruction and limiting procedure are explained.

3.1 Space discretization

Let $\mathcal{E}_h$ be a mesh composed of quadrilateral and triangular elements not necessarily conformal. For all $E \in \mathcal{E}_h$. We define h_E the diameter of the element $E \in \mathcal{E}_h$ as the ratio between its surface and perimeter.

The set of all open faces of all elements $E \in \mathcal{E}_h$ is denoted by $\mathcal{F}_h$. Moreover, we can define two subsets of $\mathcal{F}_h$, $\mathcal{F}_h^\partial$ for the boundary faces and $\mathcal{F}_h^{in}$ for the interior faces:

$$\mathcal{F}_h^\partial := \bigcup_{F \in \partial\Omega} F \quad \text{and} \quad \mathcal{F}_h^{in} := \mathcal{F}_h \backslash \mathcal{F}_h^\partial.$$

For a given $E \in \mathcal{E}_h$, there exists a set of face $\mathcal{F}_h^E := \{F \in \mathcal{F}_h, F \in \partial E\}$. For all $F \in \mathcal{F}_h^E \cap \mathcal{F}_h^{in}$, there exists a neighboring element E_r such that $E \cap E_r = F$ and we define the normal unit vector $\vec{n}_{E,F} := (n_x, n_y)^T$ pointing from E to E_r. For all $F \in \mathcal{F}_h^E \cap \mathcal{F}_h^\partial$, there exists E_∂ a fictitious element such that $E \cap E_\partial = F$ and we define the normal unit vector $\vec{n}_{E,F}$ pointing always from E to E_∂.

Firstly the space $\mathbb{P}^p(E)$ with $p \in \mathbb{N}$ and $E \in \mathcal{E}_h$ is the space of polynomial functions of two variables over E and of degree p at most. The goal is to find the approximation vector on each element of $\mathcal{E}_h$, hence the solution space is defined as $\mathbb{P}_h^p := \{v : \Omega \to \mathbb{R} : v_{|_E} \in \mathbb{P}^p(E),\ \forall E \in \mathcal{E}_h\}$.

Equations (1) are multiplied by a test function $\varphi_h \in [\mathbb{P}_h(E)]^3$, then they are integrated over E and finally Green's formula is applied. It gives the continuous-in-time space approximation :

$$\begin{aligned} &\text{Find } U_h := (\zeta_h, (q_x)_h, (q_y)_h) \in [\mathbb{P}_h(E)]^3 \text{ such that } \forall t \in]0, T[,\ \forall E \in \mathcal{E}_h \text{ and } \forall \varphi_h \in [\mathbb{P}_h(E)]^3, \\ &\begin{cases} \displaystyle\int_E \varphi_h \frac{\partial U_h}{\partial t} - \int_E \nabla\varphi_h : \mathbb{G}(U_h)^t + \sum_{F \in \mathcal{F}_h^E} \int_F \varphi_h \hat{G}_F(U_h) = \int_E \varphi_h \mathbb{S}(U_h, z_h) \\ \textit{Initial condition,} \end{cases} \end{aligned} \tag{2}$$

where z_h is the projection of the bathymetry z onto the DG space and $\hat{G}_F$ is the numerical flux across F. The numerical flux is defined as follows:

$\forall F \in \mathcal{F}_h, \forall (x,y) \in F,$

$$\hat{G}_F(U_h)(x,y) = \begin{cases} \tilde{G}\Big(U_h|_E(x,y), U_h|_{E_r}(x,y), \vec{n}_{E,F}\Big), & \text{if} \quad F \in \mathcal{F}_h^{in} \\ \tilde{G}\Big(U_h|_E(x,y), U_h|_{E_\partial}(x,y), \vec{n}_{E,F}\Big), & \text{if} \quad F \in \mathcal{F}_h^{\partial} \end{cases} \tag{3}$$

where $\tilde{G}$ is the numerical flux function independent of the face. $U_h|_{E_\partial}(x,y)$ is used to enforce boundary conditions weakly through the numerical fluxes. Moreover $\tilde{G}$ has to be *conservative* and *consistent*. In this work, the global Lax-Friedrich approximation is used to evaluate $\tilde{G}$ at every $F \in \mathcal{F}_h$ or the Godunov scheme solving a Riemann problem at the interface.

We take $\mathbb{P}_h^p$ as DG space, so U_h and φ_h can be expressed as a linear combination of polynomials. There exist many choices for the polynomials basis, monomial, Lagrange, Dubiner [14], or Legendre basis. In this work the Legendre (resp. Dubiner) polynomials basis is used for quadrilateral (resp. triangular) elements. Those basis are orthogonal and hold the hierarchism property, i.e. mass matrix is diagonal and the polynomial degree can be increased or decreased effortlessly.

Classically in Finite Element methods each element is mapped on a reference element $\hat{E}$ with local variables ξ and η. The polynomial approximation is defined on this reference element. For instance for quadrilateral elements a tensor-product basis is constructed using the Legendre polynomial basis.

$$U_h|_{\hat{E}}(\xi,\eta,t) = \sum_{i=1}^{p}\sum_{j=1}^{p} (\mathbf{U}_{\hat{E}})_{i,j}(t) P_i(\xi) P_j(\eta), \quad \forall (\xi,\eta,t) \in \hat{E} \times]0,T[\tag{4}$$

where P is the Legendre polynomial vector which order is lower than p. $\mathbf{U}_{\hat{E}} \in [\mathbb{R}^3]^{(p+1)\times(p+1)}$ is the local expansion coefficient matrix with $(U_{\hat{E}})_{i,j} = ((\zeta_{\hat{E}})_{i,j}, (q_{x\hat{E}})_{i,j}, (q_{y\hat{E}})_{i,j})$.

In practice, for all element E, the coefficients of $\mathbf{U}_{\hat{E}}$ are stored in a unique vector $\vec{U}_{\hat{E}} \in [R^3]^N$ with $N = (p+1)^2$ the number of degree of freedom per element per unknown. Moreover, polynomial basis functions are stored the same way in a vector Φ. Hence it gives

$$U_h|_{\hat{E}}(\xi,\eta,t) = \Phi(\xi,\eta) \cdot \vec{U}_{\hat{E}}(t), \quad \forall (\xi,\eta,t) \in \hat{E} \times]0,T[. \tag{5}$$

We obtain a discrete form of the variational problem (2) for an element E and its corresponding $\hat{E}$:

$$\int_{\hat{E}} \Phi \otimes \Phi \frac{\partial \vec{U}_{\hat{E}}}{\partial t} - \int_{\hat{E}} \nabla\Phi : \mathbb{G}(U_h)^t + \sum_{\hat{F} \in \mathcal{F}_h^{\hat{E}}} \int_{\hat{F}} \Phi \hat{G}_{\hat{F}}(U_h) = \int_{\hat{E}} \Phi \mathbb{S}(U_h, z_h). \tag{6}$$

Then by inverting the mass matrix in (6), which is diagonal thanks to orthogonal chosen basis, we can write:

$$\text{Solve } \forall E \in \mathcal{E}_h, \frac{d\vec{U}_{\hat{E}}}{dt} = \mathcal{H}_h(\vec{U}_{\hat{E}}) \tag{7}$$

where $\mathcal{H}_h : [R^3]^N \to [R^3]^N$.

3.2 Time discretization

The time derivative in (7) is discretized using the explicit Runge-Kutta method of order q, considering $(t^k)_{k\in\mathbb{N}}$ a sequence of discrete times beginning at $t^0 = 0$ and $(\Delta t)^k := t^{k+1} - t^k$ the $(k+1)$-th time step. Given an initial condition U_0, the RK method reads to compute the solution at t^{k+1}, using the solution U^k at t^k and some sub-iterate solutions between t^k and t^{k+1}:

$$\vec{U}_{\hat{E}}^{k+1} = \vec{U}_{\hat{E}}^{k} + (\Delta t)^k \sum_{i=1}^{q} b_i k_i, \tag{8}$$

$$\text{with} \begin{cases} k_1 = \mathcal{H}_h(\vec{U}_{\hat{E}}^{k}) \\ k_i = \mathcal{H}_h(\vec{U}_{\hat{E}}^{k} + (\Delta t)^k \sum_{j=1}^{i-1} a_{i,j} k_j) \end{cases} . \tag{9}$$

Coefficients $a_{i,j}$ and b_i can be found in [7]. In order to reach the same order of accuracy in space and time we use a Runge-Kutta method of order $p+1$.

The time step is determined according to a CFL condition [7]:

$$\max_{E\in\mathcal{E}_h}\left(\frac{\lambda_E^k}{h_E}\right)(\Delta t)^k \leq \frac{1}{2p+1},$$

with

$$\lambda_E^k := \max_{F\in\partial E}\Big(\max_{(x,y)\in F}\Big((\frac{q_x}{\zeta}n_x + \frac{q_y}{\zeta}n_y \pm \sqrt{g\zeta}\big)(x,y,t^k)\Big)\Big).$$

3.3 Well balanced property

Solving SWE with bathymetry with (2) does not preserve equilibrium states. The RKDG method is not well-balanced. It generates some numerical waves that decrease the accuracy of the approximation scheme, because of an incompatibility between the numerical flux and the discretization of the source term.

The *lake at rest* equilibrium needs to be conserved, therefore the problem (1) is modified, hence (2), in order to obtain a well-balanced RKDG scheme [10].

Firstly it can be that noticed we cannot have $\zeta_h + z \equiv C$ because z does not belong to $\mathbb{P}_h^p$. Therefore, we need to find $z_h \in \mathbb{P}_h^p$, the L^2-projection of z onto $\mathbb{P}_h^p$ such that $\zeta_h + z_h \equiv C$.

The well-balanced RKDG formulation now reads:

$$\int_E \varphi_h \frac{\partial U_h}{\partial_t} - \int_E \nabla\varphi_h : \mathbb{G}(U_h)^t + \sum_{F\in\mathcal{F}_h^E}\int_F \varphi_h\big(\hat{G}_F(U_h^\diamond) - \delta_F(U_h, z_h)\big) = \int_E \varphi_h \mathbb{S}(U_h, z_h) \tag{10}$$

with $U_h^\diamond := (\zeta_h^\diamond, \mathbf{q}_h^\diamond)$ the modified flux. For all $F \in \mathcal{F}_h$ we define:

$$\zeta_h^\diamond|_E := \begin{cases} \max\big(0, \zeta_h|_E - \max(z_h|_{E_r} - z_h|_E, 0)\big) & , \quad \text{if } F \in \mathcal{F}_h^{in} \\ \zeta|_E & , \quad \text{if } F \in \mathcal{F}_h^{\partial} \end{cases}, \ \mathbf{q}_h^\diamond := \zeta_h^\diamond|_E \frac{\mathbf{q}_h^\diamond|_E}{\zeta_h|_E} \tag{11}$$

The additional source term on the interfaces is defined:

$$\delta_F(U_h, z_h) := \begin{pmatrix} 0 \\ \frac{g}{2}(\zeta_h^\diamond|_E^2 - \zeta_h|_E^2)n_x \\ \frac{g}{2}(\zeta_h^\diamond|_E^2 - \zeta_h|_E^2)n_y \end{pmatrix} \tag{12}$$

The proof that this modification of (2) conserves the equilibrium state can be found in [10].

3.4 Limiting procedure

Limiting methods to reduce spurious oscillations are commonly used in the framework of solving SWE using RKDG method [7, 10, 11]. Unfortunately those procedures are not general and can not be applied to a general mesh.

In this work the method we described has been introduced by Krivodonova [6] in 2007 and is applied only to non-conformal mesh formed with quadrilateral elements, in this case, the mapping between elements and reference elements is linear. Nevertheless there exists a moment limiter [14] that can be applied to triangular elements.

Moment limiting does not directly reduce to first order polynomial in the spurious oscillated area. It begins by limiting the highest moments and only if they need to be limited, lower moments are limited. Using this procedure, the benefit of a DG approach is preserved as much as possible.

For an element $E \in \mathcal{E}_h$, for all $F \in \mathcal{F}_h^E$, the procedure consists in comparing the i-th (resp. j-th) derivative of $U_h|_E$ with the finite difference between the $(i-1)$-th (resp. $(j-1)$-th) derivative of $U_h|_E$ and $U_h|_{E_r}$ in the direction ξ (resp. η). The estimation of $(\mathbf{U}_{\hat{E}})_{i,j}^k$ is given by:

$$(\mathbf{U}_{\hat{E}})_{i,j}^k \approx \frac{(\mathbf{U}_{\hat{E}_r})_{i-1,j}^k - (\mathbf{U}_{\hat{E}})_{i-1,j}^k}{2\sqrt{4i^2-1}} \text{ in the direction } \xi, \tag{13}$$

and

$$(\mathbf{U}_{\hat{E}})^k_{i,j} \approx \frac{(\mathbf{U}_{\hat{E}_r})^k_{i,j-1} - (\mathbf{U}_{\hat{E}})^k_{i,j-1}}{2\sqrt{4j^2-1}} \text{ in the direction } \eta. \tag{14}$$

Further information about these approximations can be found in [6].

We are solving a non-linear system, therefore moment limiting can't be applied directly to conserved variables because it leads to spurious oscillations near discontinuities. This phenomenon is observed in [6, 15]. To achieve a better moment limiter, characteristic field decomposition needs to be achieved. That is to say we do not limit $(\mathbf{U}_{\hat{E}})^k_{i,j}$ but $(\mathbf{C}_{\hat{E}})^k_{i,j} := \mathbf{L}(\mathbf{U}_{\hat{E}})^k_{i,j}$ where $\mathbf{L}$ is the matrix of left eigenvectors of the Jacobian of (1). $\mathbf{L}$ is evaluated using an arithmetic mean of $\overline{U_h}_E$ and $\overline{U_h}_{E_r}$ defined as

$$\overline{U_h}_E = \frac{1}{\mathfrak{s}_E}\int_E U_h dS, \quad \overline{U_h}_{E_r} = \frac{1}{\mathfrak{s}_{E_r}}\int_{E_r} U_h dS.$$

At each step of the limiting procedure, for all $F \in \mathcal{F}_h^{in}$, $(\widehat{\mathbf{C}_{\hat{E}}})^k_{i,j}$ and $(\widehat{\mathbf{C}_{\hat{E}_r}})^k_{i,j}$ are defined analogously by

$$(\widehat{\mathbf{C}_{\hat{E}}})^k_{i,j} := \begin{cases} \mathbf{m}\Big((\mathbf{C}_{\hat{E}})^k_{i,j}, \alpha_i\big((\mathbf{C}_{\hat{E}_r})^k_{i-1,j} - (\mathbf{C}_{\hat{E}})^k_{i-1,j}\big)\Big), \text{ if } \vec{n}_{\hat{E},F}\cdot(0,1) = 0 \text{ and } i > 0 \\ \mathbf{m}\Big((\mathbf{C}_{\hat{E}})^k_{i,j}, \alpha_j\big((\mathbf{C}_{\hat{E}_r})^k_{i,j-1} - (\mathbf{C}_{\hat{E}})^k_{i,j-1}\big)\Big), \text{ if } \vec{n}_{\hat{E},F}\cdot(1,0) = 0 \text{ and } j > 0 \end{cases}$$

where the function $\mathbf{m}$ is defined by:

$$\forall\, a_1, a_2 \in \mathbb{R}^3,\ \mathbf{m}(a_1,a_2) := \begin{pmatrix} \text{minmod}\big((a_1)_1,(a_2)_1\big) \\ \text{minmod}\big((a_1)_2,(a_2)_2\big) \\ \text{minmod}\big((a_1)_3,(a_2)_3\big) \end{pmatrix} \tag{15}$$

with

$$\forall\, a,b \in \mathbb{R},\ \text{minmod}(a,b) = \begin{cases} \text{sgn}(a)\min(|a|,|b|) & , \text{ if sgn(a)=sgn(b)} \\ 0 & , \text{ otherwise} \end{cases}.$$

The choice of α_i and α_j is done according to (13), (14) and because we do not allow $(\mathbf{C}_{\hat{E}})^k_{i,j}$ to exceed $2(2i-1)$ times the lower derivative in ξ direction and $2(2j-1)$ times the lower derivative in η direction. It gives :

$$\frac{1}{2\sqrt{4n^2-1}} \le \alpha_n \le \sqrt{\frac{2n-1}{2n+1}}.$$

The left bound of α_n gives the most diffusive limiter and the right bound gives the least diffusive.

Once the limiting step is done we recover limited conserved variables by multiplying $(\widehat{\mathbf{C}_{\hat{E}}})^k_{i,j}$ by $\mathbf{L}^{-1}$. The whole limiting procedure is described in [6].

4 Numerical validation

In this section the RKDG method is validated using a one-dimensional dam break and its behavior with a block-based adaptive mesh refinement are tested.

4.1 Dam break on a wet domain

The dam break problem is a classical case in the shallow water community, it was introduced first in [16]. This is a classical Riemann problem. Here we consider an ideal dam break on a wet domain, i.e. the dam break is instantaneous, the bottom is flat and frictionless. The analytical solution is obtained thanks to the characteristics method and it can be found in [17, 16].

Here we consider a one-dimensional problem on a domain $\Omega = [-10, 10]$ and $t \in]0, 2]$. The initial condition considered for this problem is the following Riemann problem:

$$\forall x \in \Omega,\ \zeta(x,0) = \begin{cases} 1.8 & , \text{ if } x < 0 \\ 0.5 & , \text{ if } x \ge 0 \end{cases}, \quad \mathbf{q}(x,0) = 0. \tag{16}$$

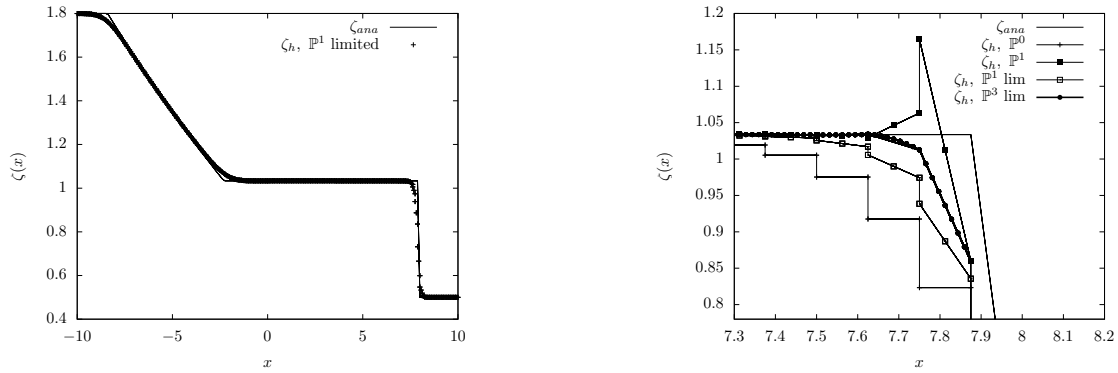

Figure 1: Water depth profile (left) and a zoom around the discontinuity (right) for the dam-break on a wet domain at $t = 2s$

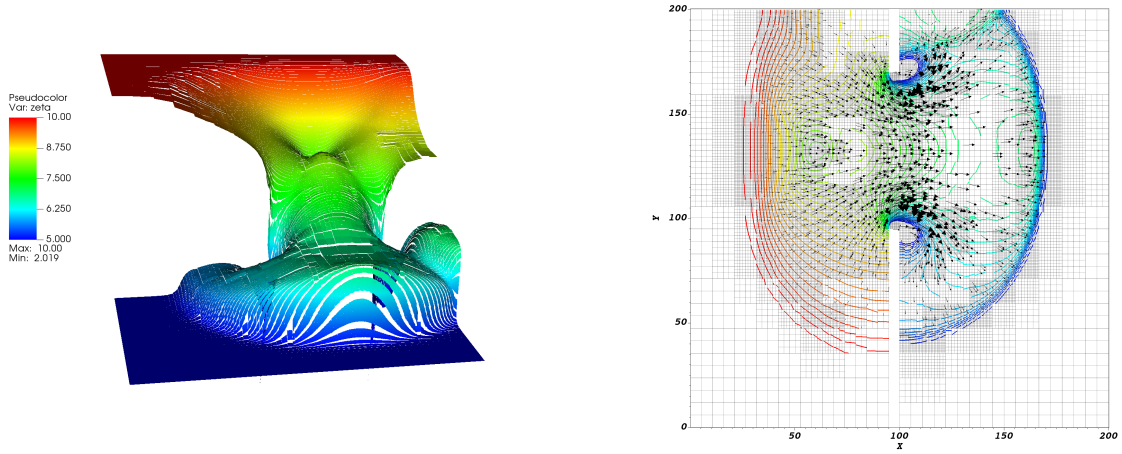

Figure 2: Water depth and depth contour with velocity field for the partial dam-break at $t = 7.2s$

The approximated solution of this problem is obtained using the RKDG method, exposed before with the moment limiting parameter α set to be the least diffusive. One can see in Figure 1 the solution computed with a mesh composed of 160 elements and a Runge-Kutta method of order $p+1$ with p the polynomial degree ($p = 0,\ 1$ and 3). On the left, there are the analytical solution on solid line and the approached solution with cross markers. It can be noticed that they overlap correctly on the whole domain but there is still diffusion near discontinuities. A zoom-in displayed on the right side of Figure 1, it can be observed that piecewise constant approximation (FV) is the most diffusive. The piecewise linear approximation (DG $\mathbb{P}^1$) without moment limiter introduces spurious oscillations and finally DG $\mathbb{P}^1$ and $\mathbb{P}^3$ with moment limiter are less diffusive than FV and does not oscillate around discontinuity. The higher order is the least diffusive.

4.2 Two-dimensional partial dam-break

This numerical validation allows us to test our solver on real $2D$ conditions. It is used to validate FV solver in [18, 19] and in [11] to validate his DG solver. This test case is an asymmetrical breach in a dam full of water. The computational domain $\Omega = [0, 200] \times [0, 200]$ and $T = 7.2s$. The breach is $75m$ long and located at $30m$ from the upper wall and $95m$ from the lower wall. The problem geometry can be seen in Figure 2. At the initial time, the dam is full of water before the breach $\zeta_l = 10m$ and the is water after the dam $\zeta_r = 5m$. Boundary conditions are all considered reflective.

The computation of the approached solution of this problem is done using the RKDG solver

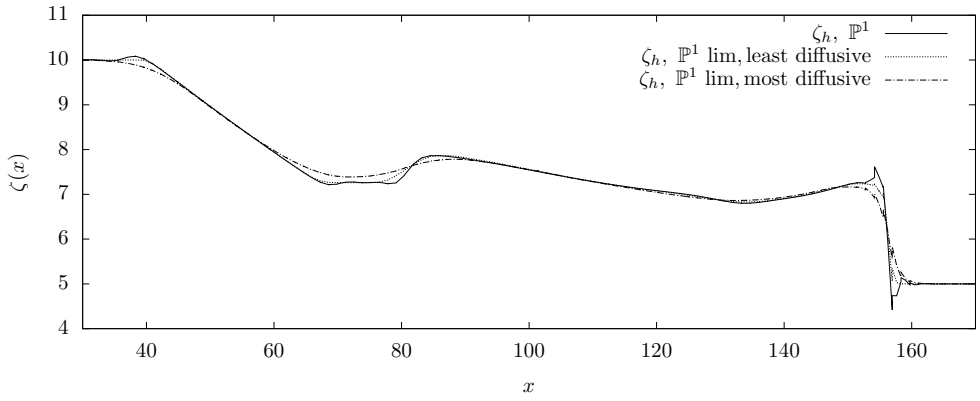

Figure 3: Water depth cross-section at $y = 132.5m$, i.e. in the middle of the breach, at $t = 6s$

exposed before with moment limiting set to be the most diffusive. In this computation, the solution is considered as a discontinuous polynomial of degree one ($\mathbb{P}^1$), hence the time integration is done with a Rung-Kutta method of order 2. In Figure 2 the water depth elevation is displayed on the left and it is in good agreement with results in [19]. Moreover, it can be seen that discontinuities are better captured using the RKDG solver. Moreover, because the solver is implemented on a non-conformal mesher to speed up computation we used a mesh refinement technique based on the gradient of ζ. It can be seen in Figure 2 that element size is not constant over the computational domain. The behavior of the approximated velocity field is as expected, there is clearly a flow from right to left with eddies around corners of the breach. In Figure 3 the water depth elevation is displayed without slope limiter (solid line), with the least diffusive slope limiter (dotted line) and with the most diffusive slope limiter (dashed line). In can be noticed that slope limiter behave as expected, it cancels oscillations near discontinuities and is more or less diffusive according to the parameter α_n.

5 Conclusion

In this paper Shallow Water Equations with bathymetry are numerically solved using Rung-Kutta Discontinuous Galerkin methods. Moreover in order to increase robustness of those methods, hydrostatic reconstruction and moment limiting are added. This whole solver is implemented in a way to be used with an adaptive mesh refinement method using a block-based approach. In order to validate the numerical simulation of Shallow Water Equations, a one-dimensional dam break problem displays the benefit of using RKDG methods with moment limiting compared to Finite Volume methods. A two-dimensional dam break problem exhibits the behavior of adaptive RKDG methods.

Acknowledgment

This work has been supported financially by *Provence-Alpes-Côte d'Azur region (France).*

References

[1] Clément, J.-B., Golay, F., Ersoy, M. & Sous, D.: An adaptive strategy for discontinuous Galerkin simulations of Richards' equation: Application to multi-materials dam wetting. *Advances in Water Resources* vol. 151: (2021)

[2] De Saint-Venant, A.J.C.B.: Théorie du mouvement non permanent des eaux, avec application aux crues des rivières et à l'introduction des marées dans leur lit. *Comptes rendus hebdomadaires des séances de l'Académie des sciences.* Gauthier-Villars, (1871).

[3] Gerbeau, J.-F. & Perthame, B.: Derivation of viscous saint-venant system for laminar shallow water; numerical validation. *Discrete and Continuous Dynamical Systems - B*, vol. 1, no. 1: (2001) pp. 89–102.

[4] Marche, F.: Derivation of a new two-dimensional viscous shallow water model with varying topography, bottom friction and capillary effects. *European Journal of Mechanics - B/Fluids*, vol. 26, no. 1: (2007) pp. 49–63.

[5] Cockburn, B. & Shu, C.-W.: TVB runge-kutta local projection discontinuous Galerkin finite element method for conservation laws II: General framework. *Mathematics of Computation*, vol. 52, no. 186: (1989) pp. 411–435.

[6] Krivodonova, L.: Limiters for high-order discontinuous Galerkin methods. *Journal of Computational Physics*, vol. 226, no. 1: (2007) pp. 879–896.

[7] Cockburn, B. & Shu, C.-W.: Runge–kutta discontinuous Galerkin methods for convection-dominated problems. *Journal of Scientific Computing*, vol. 16: (2001) pp. 173–261.

[8] Aizinger, V. & Dawson, C.: A discontinuous Galerkin method for two-dimensional flow and transport in shallow water. *Advances in Water Resources*, vol. 25, no. 1: (2002) pp. 67–84.

[9] Ambati, V. & Bokhove, O.: Space–time discontinuous Galerkin finite element method for shallow water flows. *Journal of Computational and Applied Mathematics*, vol. 204, no. 2: (2007) pp. 452–462.

[10] Ern, A., Piperno, S. & Djadel, K.: A well-balanced Runge-Kutta Discontinuous Galerkin method for the Shallow-Water Equations with flooding and drying.

[11] Duran, A. & Marche, F.: Recent advances on the discontinuous Galerkin method for shallow water equations with topography source terms. *Computers and Fluids*, vol. 101: (2014) pp. 88–104.

[12] Gottlieb, S., Shu, C.-W. & Tadmor, E.: Strong stability-preserving high-order time discretization methods. *SIAM Review*, vol. 43, no. 1: (2001) pp. 89–112.

[13] Altazin, T., Ersoy, M., Golay, F., Sous, D. & Yushchenko, L.: Numerical investigation of BB-AMR scheme using entropy production as refinement criterion. *International Journal of Computational Fluid Dynamics*, vol. 30, no. 3: (2016) pp. 256–271.

[14] Dutt, K. & Krivodonova, L.: A high-order moment limiter for the discontinuous Galerkin method on triangular meshes. *Journal of Computational Physics*, vol. 433: (2021) pp. 110188.

[15] Cockburn, B., Lin, S.-Y. & Shu, C.-W.: TVB Runge-Kutta local projection discontinuous Galerkin finite element method for conservation laws III: One-dimensional systems. *Journal of Computational Physics*, vol. 84, no. 1: (1989) pp. 90–113.

[16] Stoker, J. J.: Water waves : The Mathematical Theory with applications. *John Wiley & Sons, Ltd*, (1992) pp. 333–341.

[17] Delestre, O., Lucas, C., Ksinant, P.-A., Darboux, F., Laguerre, C., Vo, T. N. T., James, F. & Cordier, S.: Swashes: a compilation of shallow water analytic solutions for hydraulic and environmental studies. *International Journal for Numerical Methods in Fluids*, vol. 72, no. 3: (2013)

[18] Vosoughifar, H. R., Dolatshah, A. & Shokouhi, S. K. S.: Discretization of multidimensional mathematical equations of dam break phenomena using a novel approach of finite volume method. *Journal of Applied Mathematics*, vol. 2013: (2013) pp. 1–12. (2013) pp. 269–300.

[19] Delis, A. & Katsaounis, T.: Numerical solution of the two-dimensional shallow water equations by the application of relaxation methods. *Applied Mathematical Modelling*, vol. 29, no. 8: (2005) pp. 754–783.